

Ligustilide protects PC12 cells from oxygen-glucose deprivation/reoxygenation-induced apoptosis via the LKB1-AMPK-mTOR signaling pathway

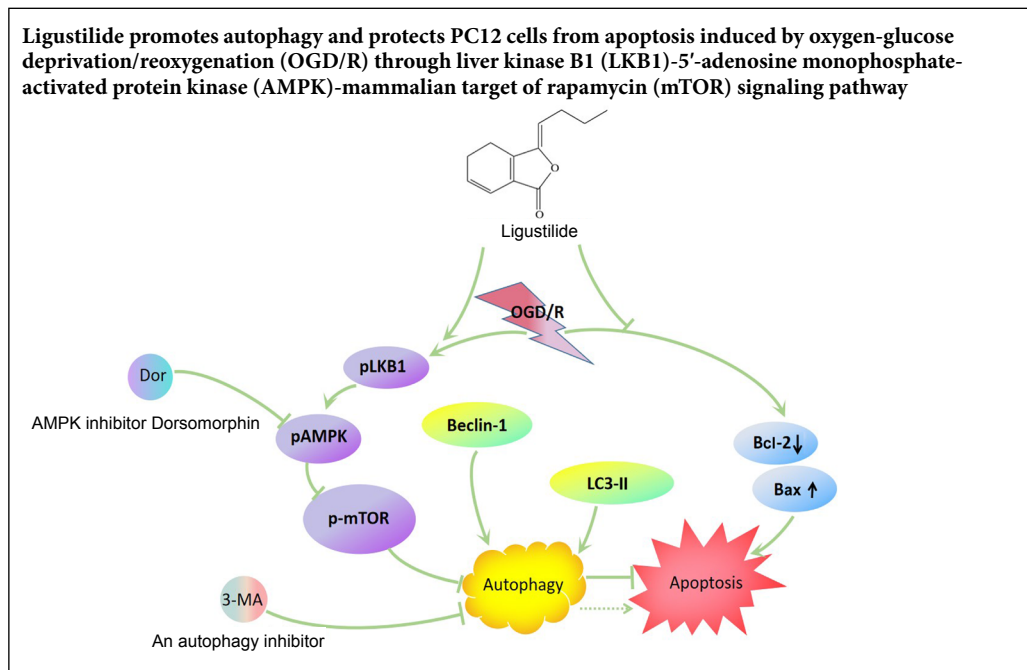
Dan-Yang Zhao^{1,2}, Dong-Dong Yu³, Li Ren², Guo-Rong Bi^{1,*}

¹ Shengjing Hospital of China Medical University, Shenyang, Liaoning Province, China

² The First People's Hospital of Shenyang, Shenyang, Liaoning Province, China

³ The First Affiliated Hospital of Liaoning University of Traditional Chinese Medicine, Shenyang, Liaoning Province, China

Graphical Abstract



*Correspondence to:

Guo-Rong Bi, MD,
bigr@sj-hospital.org.

orcid:

0000-0002-6805-4430
(Dan-Yang Zhao)

doi: 10.4103/1673-5374.266059

Received: March 2, 2019

Accepted: May 10, 2019

Abstract

Autophagy has been shown to have a protective effect against brain damage. Ligustilide (LIG) is a bioactive substance isolated from *Ligusticum chuanxiong*, a traditional Chinese medicine. LIG has a neuroprotective effect; however, it is unclear whether this neuroprotective effect involves autophagy. In this study, PC12 cells were treated with 1×10^{-5} – 1×10^{-9} M LIG for 0, 3, 12 or 24 hours, and cell proliferation was evaluated using the 3-(4,5-dimethylthiazol-2-yl)-5-(3-carboxymethoxyphenyl)-2-(4-sulfophenyl)-2H-tetrazolium (MTS) assay. Treatment with 1×10^{-6} M LIG for 3 hours had the greatest effect on cell proliferation, and was therefore used for subsequent experiments. PC12 cells were pre-treated with 1×10^{-6} M LIG for 3 hours, cultured in 95% N₂/5% CO₂ in Dulbecco's modified Eagle's medium without glucose or serum for 4 hours, and then cultured normally for 16 hours, to simulate oxygen-glucose deprivation/reoxygenation (OGD/R). Cell proliferation was assessed with the MTS assay. Apoptosis was detected by flow cytometry. The expression levels of apoptosis-related proteins, Bcl-2 and Bax, autophagy-related proteins, Beclin 1 and microtubule-associated protein I light chain 3B (LC3-II), and liver kinase B1 (LKB1)-5'-adenosine monophosphate-activated protein kinase (AMPK)-mammalian target of rapamycin (mTOR) signaling pathway-related proteins were assessed by western blot assay. Immunofluorescence staining was used to detect LC3-II expression. Autophagosome formation was observed by electron microscopy. LIG significantly decreased apoptosis, increased Bcl-2, Beclin 1 and LC3-II expression, decreased Bax expression, increased LC3-II immunoreactivity and the number of autophagosomes, and activated the LKB1-AMPK-mTOR signaling pathway in PC12 cells exposed to OGD/R. The addition of the autophagy inhibitor 3-methyladenine or dorsomorphin before OGD/R attenuated the activation of the LKB1-AMPK-mTOR signaling pathway in cells treated with LIG. Taken together, our findings show that LIG promotes autophagy and protects PC12 cells from apoptosis induced by OGD/R via the LKB1-AMPK-mTOR signaling pathway.

Key Words: AMPK; apoptosis; autophagy; Bax; Bcl-2; Beclin 1; LC3-II; ligustilide; mTOR; PC12 cells

Chinese Library Classification No. R453; R932; R741

Introduction

Stroke is the main cause of neurological disability (Siniscalchi et al., 2014), and ischemic cerebral infarction (ICI) comprises approximately 80–85% of all strokes (Qian et al., 2018). The current standard treatment for ischemia is rapid reperfusion; however, ischemia/reperfusion aggravates brain tissue damage. Studies show that autophagy and apoptosis play critical roles in hypoxia-induced ICI (Yousuf et al., 2009; Descloux et al., 2015). In the central nervous system, autophagy is activated by various factors, including ischemia and hypoxia (Gabryel et al., 2012). Deficiency of the autophagy-related gene *Atg7* causes massive neuronal loss in the cerebral and cerebellar cortices, which exacerbates neurodegeneration (Komatsu et al., 2006). Recent studies show that enhancing autophagy has a protective effect against brain damage (Shen et al., 2016; Dai et al., 2017). However, excessive autophagy can induce cellular dysfunction or cell death (Rami et al., 2008).

Ligustilide (LIG) is a bioactive substance isolated from *Ligusticum chuanxiong*. LIG protects cells and functions as an autophagy inhibitor to overcome chemoresistance in breast cancer cells by regulating the autophagic process (Shi et al., 2015; Qi et al., 2017). LIG has been found to have a neuroprotective effect as well (Yu et al., 2015; Qi et al., 2017; Byun et al., 2018). LIG protects against Alzheimer's disease by inducing autophagy via inhibition of the protein kinase B (PKB/Akt)/mammalian target of rapamycin (mTOR) pathway (Kuang et al., 2017).

The PC12 cell line is derived from a pheochromocytoma of the rat adrenal medulla, and exhibits characteristics of neural cells (Zhu et al., 2010). Oxygen-glucose deprivation/reoxygenation (OGD/R) is widely used to simulate neuronal ischemia/reperfusion injury (Ecker et al., 2010). At present, it is not clear whether LIG can inhibit apoptosis through autophagy. Therefore, in this study, we investigated the effect of LIG on autophagy in PC12 cells exposed to OGD/R.

Materials and Methods

Cell lines and culture

PC12 cells were kindly provided by the Experimental center of Affiliated Hospital of Liaoning University of Traditional Chinese Medicine, Shenyang, China. PC12 cells were maintained in 75-mL vented culture flasks using high-glucose Dulbecco's modified Eagle's medium with pyruvate and supplemented with 5% (v/v) fetal bovine serum, 10% (v/v) horse serum, 100 U/mL penicillin and 100 µg/mL streptomycin at 37°C in a humidified incubator with a 5% CO₂/95% air atmosphere (Ahn et al., 2004). PC12 cells were incubated with 50 ng/mL nerve growth factor (Gibco, Grand Island, NY, USA) for 24 hours to induce neurite formation to mimic neuronal cells (Klein et al., 2007). The medium was changed every 3 days. Cells reached 60–70% confluence after 5–6 days of incubation in the flask. To investigate whether LIG could induce autophagy, the cells were divided into five groups: control, OGD/R, LIG + OGD/R, 3-methyladenine (3-MA) + OGD/R, and LIG + 3-MA + OGD/R. Addition of 3-MA, an autophagy inhibitor, was used to evaluate whether LIG exerts neuroprotective effects by regulating autophagy.

Production of the OGD/R model

To model ischemia/reperfusion-like conditions *in vitro*, PC12 cells were incubated in an anaerobic chamber, HER-Acell 150 (Biotech, Oxford, UK), and maintained in pre-warmed, glucose and serum-free Dulbecco's modified Eagle's medium at 37°C and 52 mmHg partial oxygen pressure. The residual oxygen was removed with an anaerobic gas mix (95% N₂, 5% CO₂) bubbled for 30 minutes into the chamber. To produce the OGD/R model, the cells were incubated in this solution at 37°C for a 4-hour period, and then re-oxygenated (returned to the normal aerobic environment for another 16 hours) (Klein et al., 2007).

3-MA, dorsomorphin and LIG treatment

The cells were treated with 3-MA (5 mM; Selleck, Houston, TX, USA) for 1 hour, which inhibits autophagy. The cells were treated for 0, 3, 12 or 24 hours with 1×10^{-5} – 1×10^{-9} M LIG. The 5'-adenosine monophosphate-activated protein kinase (AMPK) inhibitor dorsomorphin (10 µM; Selleck; treated for 30 minutes) was added to inhibit the AMPK pathway (Rao et al., 2016). In the LIG + 3-MA + OGD/R group, the cells were pretreated with 3-MA (5 mM) for 1 hour, followed by a 3-hour treatment with LIG (1×10^{-6} M), and then subjected to OGD/R. For cells used for apoptosis detection, we added dorsomorphin to assess the role of the AMPK pathway. In the 3-MA + dorsomorphin + LIG + OGD/R group, the cells were pretreated with 3-MA (5 mM) for 1 hour, followed by LIG (1×10^{-6} M) for 3 hours, and then dorsomorphin (10 µM) for 30 minutes. These cells were thereafter subjected to OGD/R.

3-(4,5-Dimethylthiazol-2-yl)-5-(3-carboxymethoxyphenyl)-2-(4-sulfophenyl)-2H-tetrazolium (MTS) assay

The proliferative activity of cells was detected with an MTS kit (CellTiter 96 AQueous One Solution Cell Proliferation Assay, #G5421, Promega, Madison, WI, USA). The PC12 cells were seeded at a density of 5×10^3 cells into two sterile 96-well plates. After treatment with LIG prior to OGD/R incubation, 10 µL MTS was added to each well. The cells were treated with 5% CO₂ for 2 hours at 37°C, and then, the plate was placed on a shaker for 1 minute, and the optical density was measured at 450 nm.

Flow cytometry analysis

Apoptosis was analyzed by flow cytometry (BD Biosciences, Franklin Lakes, NJ, USA). The cells were rinsed with cold phosphate-buffered saline and resuspended in 1× binding buffer solution to a concentration of 1×10^6 cells/mL. Then, 5 µL fluorochrome-labeled Annexin V and 5 µL propidium iodide were added to the cells in a final volume of 100 µL (1×10^5 cells) in a 5 mL culture tube. The cells were gently vortexed and placed at room temperature (25°C) in the dark for 15 minutes. Thereafter, 400 µL of 1× binding buffer solution was added to each tube, and the cells were analyzed by flow cytometry (BD Biosciences) within 1 hour.

Immunofluorescence staining

Briefly, the cells in each group were plated onto coverslips and cultured overnight with or without LIG. Afterwards, the

cells were fixed with 4% paraformaldehyde (Beyotime, Wuhan, China) for 40 minutes at room temperature and washed with phosphate-buffered saline containing 0.1% Triton X-100 (Beyotime). The cells were incubated with primary antibodies (rabbit anti-microtubule-associated protein 1 light chain 3B (LC3-II) polyclonal antibody; 1:400; #ab48394, Abcam, Cambridge, UK) overnight, followed by Cy3-conjugated goat anti-rabbit IgG (1:400; #A0516, Beyotime) at 37°C for 1 hour. The cells were imaged under a confocal microscope (Olympus, Tokyo, Japan) and analyzed using Image J software (NIH, Bethesda, Maryland, USA).

Western blot analysis

The PC12 cells were extracted in RIPA lysis buffer (Beyotime) according to the manufacturer's instructions. The lysates were then centrifuged at 12,000 r/min for 10 minutes at 4°C, and the supernatants were collected. The concentration of the protein was quantified with a bicinchoninic acid protein assay kit (Beyotime). Equal amounts of protein were mixed with loading buffer (4:1) and heated at 95–100°C for 20 minutes. The samples were then resolved by sodium dodecyl sulfate polyacrylamide gel electrophoresis and transferred to polyvinylidene difluoride membranes (Millipore, Burlington, MA, USA). The membranes were blocked with 5% nonfat milk in phosphate-buffered saline for 1 hour at room temperature and then incubated with primary antibodies (rabbit anti-rat AMPK monoclonal antibody (1:600; #ab32047), rabbit anti-rat p-AMPK monoclonal antibody (1:600; #ab131357), rabbit anti-rat liver kinase B1 (LKB1) monoclonal antibody (1:600; #ab199970), rabbit anti-rat p-LKB1 monoclonal antibody (1:600; ab199970), rabbit anti-rat Beclin 1 monoclonal antibody (1:500; #ab210498), rabbit anti-rat p-LKB1 monoclonal antibody (1:500; #ab210498), rabbit anti-rat LC3-I/II monoclonal antibody (1:500; #ab168831), rabbit anti-rat p-LKB1 monoclonal antibody (1:500; #ab168831), rabbit anti-rat mTOR monoclonal antibody (1:500; #2972), rabbit anti-rat p-mTOR monoclonal antibody (1:500; #5536) or rabbit anti-rat β -actin monoclonal antibody (1:1,000; #3700); all antibodies were from Cell Signaling Technology, Danvers, MA, USA) overnight at 4°C. Immunoreactive bands were detected by incubating with horseradish peroxidase-conjugated secondary antibodies (goat anti-rabbit IgG; 1:1,000; #ab205718, Abcam) at room temperature for 1 hour. The blots were developed with a chemiluminescent substrate reagent kit (Invitrogen, Carlsbad, CA, USA). The absorbance ratio of each protein to the internal reference was used to represent the relative amount of the target protein. The optical density of each band was analyzed with a Gel Pro Analyzer 6.0 (Media Cybernetics, Bethesda, MD, USA).

Electron microscopy

PC12 cells were fixed with 2% glutaraldehyde for 2 hours, and then fixed with 1% OsO₄ for 1.5 hours at 48°C. The samples were washed and dehydrated with a graded alcohol series. The cells were infiltrated and embedded in 618 epoxy resin after dehydration, stained with uranyl acetate and lead citrate, and then examined under the transmission electron microscope (H7650, Hitachi, Tokyo, Japan).

Statistical analysis

Statistical analysis was performed using the SPSS 17.0 software package (SPSS Inc., Chicago, IL, USA). All data were presented as the mean \pm standard deviation (SD). Statistical analyses were performed using one-way analysis of variance. Further comparisons between two groups were performed with Dunnett's test. $P < 0.05$ was considered statistically significant.

Results

LIG promotes the proliferation of PC12 cells

To assess the effect of LIG on the proliferation of PC12 cells, the cells were treated with different concentrations of LIG for 0, 3, 12 and 24 hours. MTS results showed that LIG treatment increased cell growth and viability at the different time points ($P < 0.01$, vs. control group). A 3- and 12-hour intervention with LIG (1×10^{-5} , 1×10^{-6} , 1×10^{-7} M) significantly increased cell proliferative activity. Notably, treatment with 1×10^{-6} M LIG for 3 hours resulted in the highest proliferation rate (Figure 1). Therefore, a 3-hour pre-treatment with LIG (1×10^{-6} M) was used for the following experiments.

LIG reduces the OGD/R-induced inhibition of PC12 cell proliferative activity

MTS results showed that the proliferation of PC12 cells was inhibited by OGD/R in a time-dependent manner. After 3 hours of OGD/R, cell proliferative activity was inhibited by $20 \pm 1.4\%$ ($P < 0.05$, vs. control group), and after 24 hours, it was inhibited by $50 \pm 1.8\%$ ($P < 0.01$, vs. control group). Pre-treatment with LIG (1×10^{-6} M, 3 hours) significantly diminished this OGD/R-induced inhibition of cell proliferative activity. We used 3-MA to examine the role of autophagy in this process. The inhibition of cell proliferation was increased by 3-MA ($P < 0.05$, vs. control group). Furthermore, 3-MA reduced the ability of LIG to mitigate the inhibition of cell proliferative activity, although it remained higher than in cells treated with 3-MA alone ($P < 0.05$). The results showed that autophagy participated in the cytoprotective effect of LIG (Figure 2).

LIG reduced OGD/R-induced PC12 cells apoptosis

The morphological changes of PC12 cells after OGD/R were observed by inverted phase contrast microscopy. The normal PC12 cells showed neuron cell morphology, long spindle shape, and the cell body became polygonal. The longer processes of cells were interwoven into a network. The cells have uniform light transmittance and closely adhered to the bottom of the culture bottle (Mo et al., 2017; Zhang et al., 2017). After 3 hours of OGD/R, the light transmittance of the cells began to decrease, the antennae of the cells were slightly retracted, and the degree of attachment to the bottom of the bottle decreased significantly. With the prolong of OGD/R incubation, the light transmittance of the cells was further reduced, the dead cells became round and floated off the bottom in the medium (Figure 3).

Flow cytometry detected the PC12 cells apoptosis. The results showed that PC12 cells began to apoptosis after induction of 3 hours, and OGD/R can induce the apoptosis of PC12 cells in a time dependent manner. LIG significantly

reduced the apoptosis of OGD/R-induced PC12 cells ($P < 0.05$, vs. non-LIG group; **Figure 4**).

LIG reduces OGD/R-induced apoptosis of PC12 cells through the mitochondrial pathway

To further elucidate the mechanisms by which LIG inhibits apoptosis of PC12 cells induced by OGD/R, we examined the expression of Bcl-2 and Bax. Bax expression gradually increased after OGD/R, but was inhibited by LIG ($P < 0.05$ or $P < 0.01$, vs. non-LIG-group). The expression of Bcl-2 decreased after OGD/R, but was increased by LIG ($P < 0.05$ or $P < 0.01$, vs. non-LIG-group). These findings indicate that LIG inhibits apoptosis of PC12 cells induced by OGD/R through the mitochondrial pathway (**Figure 5**).

LIG simultaneously increases autophagy and inhibits apoptosis

Given that LIG inhibits OGD/R-induced PC12 cell apoptosis, we investigated the role of autophagy in this process by examining expression of LC3-II and Beclin 1. In the groups not treated with LIG, the expression of LC3-II protein increased slightly and gradually over time after OGD/R. In the LIG group, the expression of LC3-II, the main autophagy protein (Zhu et al., 2018), increased significantly ($P < 0.05$, vs. non-LIG-group). These results suggest that OGD/R weakly induces autophagy in PC12 cells, and that pretreatment with LIG significantly increases autophagy (**Figure 6**). Beclin 1 has a critical role in signaling the onset of autophagy (Kaverina et al., 2018). We found that Beclin 1 expression in the LIG group also increased significantly compared with the OGD/R group ($P < 0.05$, vs. non-LIG-group) (**Figure 6**). Thus, LIG simultaneously increases autophagy and reduces apoptosis.

To assess whether LIG increases LC3-II expression by increasing autophagy, we treated the cells with 5 mM 3-MA for 1 hour and then measured LC3-II expression. LC3-II levels were increased in the OGD/R and LIG + OGD/R groups ($P < 0.05$, vs. control group), and after 3-MA treatment, the expression of LC3-II diminished compared with the LIG + OGD/R group ($P < 0.01$). When 3-MA was combined with LIG, the expression of LC3-II diminished compared with the LIG + OGD/R group, but was higher than in the OGD/R group (**Figure 7**).

To further confirm that LIG regulates autophagy, immunofluorescence staining for LC3-II was performed to detect autophagosomes. This revealed accumulation of LC3-II around the nucleus following OGD/R. The expression of LC3-II was notably enhanced by LIG treatment. The autophagy inhibitor 3-MA reduced LC3-II immunolabeling compared with the OGD/R group. When 3-MA was combined with LIG, LC3-II immunolabeling was reduced compared with the LIG group. In summary, these findings demonstrate that LIG increases LC3-II release (**Figure 8**).

LIG increases the formation of autophagosomes

Transmission electron microscopy was used to examine the structure of the autophagosomes. The LIG group had more autophagosomes, which are double-membrane structures, compared with the OGD/R, 3-MA + OGD/R or LIG + 3-MA

+ OGD/R group ($P < 0.01$ or $P < 0.05$). These results show that LIG upregulates autophagy in the PC12 cell line (**Figure 9**).

LIG attenuates OGD/R-induced apoptosis by upregulating autophagy

PC12 cells underwent apoptosis following OGD/R for 12 h. Pretreatment with LIG significantly decreased apoptosis ($P < 0.01$, vs. control, OGD/R and 3-MA + OGD/R groups). After inhibition of autophagy with 3-MA (5 mM, 1 hour), the apoptosis rate increased significantly, and the protective effect of LIG against OGD/R diminished, compared with the OGD/R group. Next, we used the AMPK inhibitor dorsomorphin to examine the role of the LKB1-AMPK-mTOR signaling pathway in OGD/R-induced apoptosis. After treatment with 10 μ M dorsomorphin for 30 minutes, the apoptosis rate significantly increased ($P < 0.01$, dorsomorphin + OGD/R group vs. OGD/R group). The apoptosis rate in the Dor + 3-MA + LIG + OGD/R group was up by $8.5 \pm 0.08\%$, and the protective effect of LIG was diminished ($P < 0.01$, vs. LIG + OGD/R group). These results demonstrate the key role of autophagy in the neuroprotective effect of LIG (**Figure 10**).

LIG upregulates autophagy through the LKB1-AMPK-mTOR pathway

AMPK is a positive regulator of autophagy via mTOR or ULK1 (Ecker et al., 2010). AMPK activation (phosphorylation) was significantly increased in the LIG + OGD/R group ($P < 0.01$, vs. control and 3-MA + OGD/R groups). The activity of AMPK is known to be regulated by an upstream kinase, LKB1. We therefore examined LKB1 phosphorylation, and found that similar to AMPK, LKB1 phosphorylation was also significantly enhanced in the LIG + OGD/R group. This suggests that LIG upregulates the activities of LKB1 and AMPK. Additionally, mTOR phosphorylation was reduced in the LIG + OGD/R group (**Figure 11**). These findings further suggest that LIG increases autophagy via the LKB1-AMPK-mTOR signaling pathway.

Discussion

ICI is caused by insufficient oxygen supply to the nervous system (Kuang et al., 2017; Qiao et al., 2018; Rana et al., 2018; Long et al., 2019), and is accompanied by a series of neurological events (Tobin et al., 2014; Li et al., 2017b; Suda and Kimura, 2019) that lead to irreversible damage of neural cells through autophagy, necrosis and apoptosis (Fayaz et al., 2014; Fan et al., 2016). LIG is the main fat-soluble component of *Ligusticum chuanxiong*, a Chinese herbal medicine, and can quickly cross the blood-brain barrier (Shi et al., 2015). LIG has antioxidant and anti-apoptotic activities, which are thought to contribute to the neuroprotective effect of the compound (Yu et al., 2015; Byun et al., 2018). LIG protects neuronal fibers, overcomes chemoresistance and protects against AD by regulating the autophagic process (Kuang et al., 2017; Qi et al., 2017).

In this study, we investigated whether LIG regulates neuronal apoptosis through autophagy, thereby protecting neurons in ICI. We found that LIG reduced OGD/R-induced inhibition of PC12 cell proliferation and inhibited OGD/R

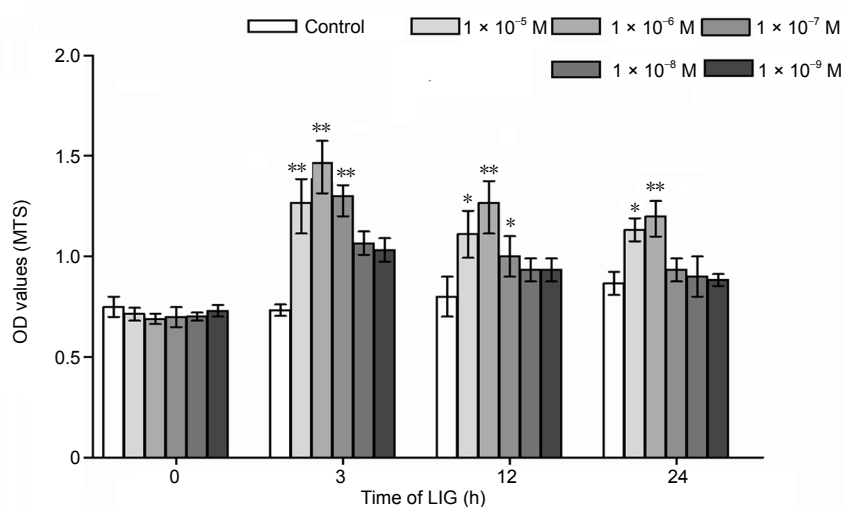


Figure 1 LIG promotes the proliferation of PC12 cells.

The cells were treated with different concentrations (1×10^{-5} – 1×10^{-9}) of LIG for 0, 3, 12 or 24 hours. Data are expressed as the mean \pm SD. * $P < 0.05$, ** $P < 0.01$, vs. control group (one-way analysis of variance followed by Dunnett's test). Experiments were repeated at least three times. LIG: Ligustilide; MTS: 3-(4,5-dimethylthiazol-2-yl)-5-(3-carboxymethoxyphenyl)-2-(4-sulfophenyl)-2H-tetrazolium; OD: optical density.

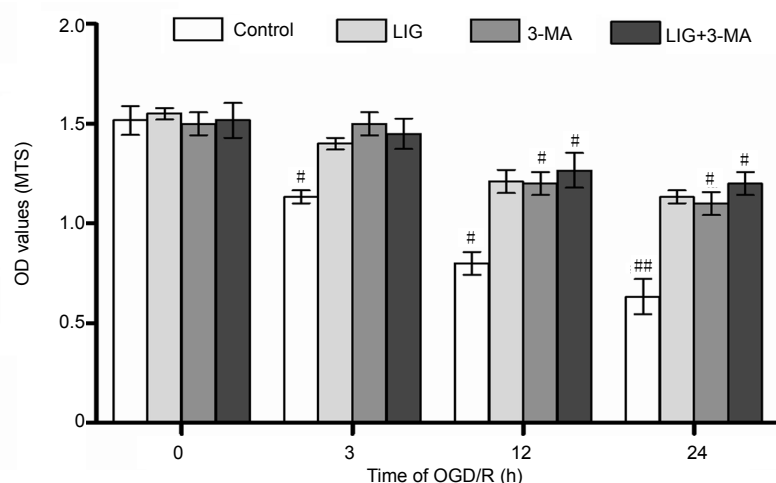


Figure 2 LIG reduces the OGD/R-induced inhibition of PC12 cell proliferative activity.

The four experimental groups included control, LIG, 3-MA and LIG + 3-MA groups. The cells were subjected to OGD/R for 0, 3, 12 or 24 hours. Data are expressed as the mean \pm SD. # $P < 0.05$, ## $P < 0.01$, vs. LIG group (one-way analysis of variance followed by Dunnett's test). Experiments were repeated at least three times. 3-MA: 3-Methyladenine; LIG: ligustilide; MTS: 3-(4,5-dimethylthiazol-2-yl)-5-(3-carboxymethoxyphenyl)-2-(4-sulfophenyl)-2H-tetrazolium; OD: optical density; OGD/R: oxygen-glucose deprivation/reoxygenation.

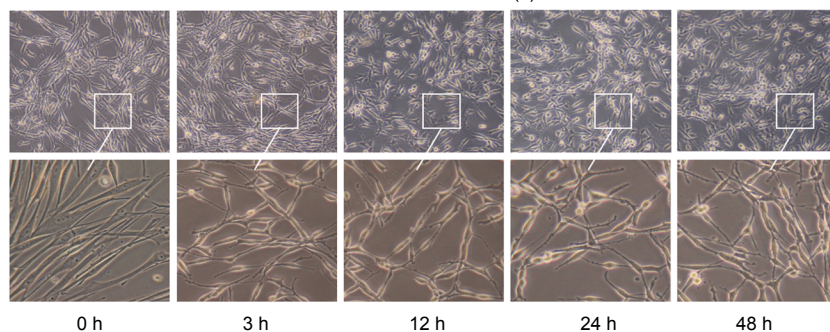


Figure 3 Effect of LIG on the morphological changes in PC12 cells exposed to OGD/R.

The morphological changes in PC12 cells after OGD/R were observed by inverted phase contrast microscopy. With the increase in OGD/R time, the dead cells became round and floated off the bottom of the culture dish. The cells were subjected to OGD/R for 0, 3, 12, 24 or 48 hours. Original magnification, upper panel: 10 \times , lower panel: 40 \times . LIG: Ligustilide; OGD/R: oxygen-glucose deprivation/reoxygenation.

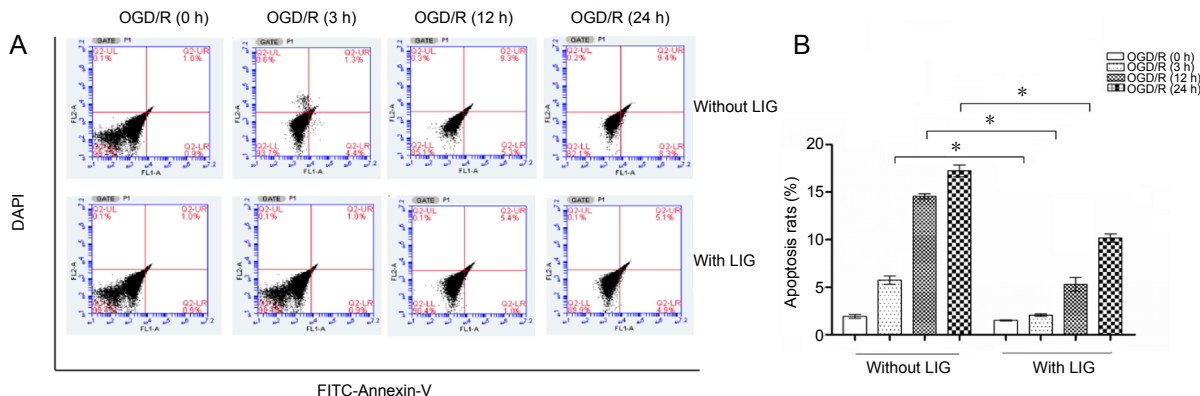


Figure 4 Effect of LIG on the apoptosis of PC12 cells exposed to OGD/R.

(A) Flow cytometry detection of PC12 cell apoptosis. (B) Quantitation of the apoptotic data. Data are expressed as the mean \pm SD. * $P < 0.05$ (one-way analysis of variance followed by Dunnett's test). Experiments were repeated at least three times. DAPI: 4',6-Diamidino-2-phenylindole; FITC: fluorescein; LIG: ligustilide; OGD/R: oxygen-glucose deprivation/reoxygenation.

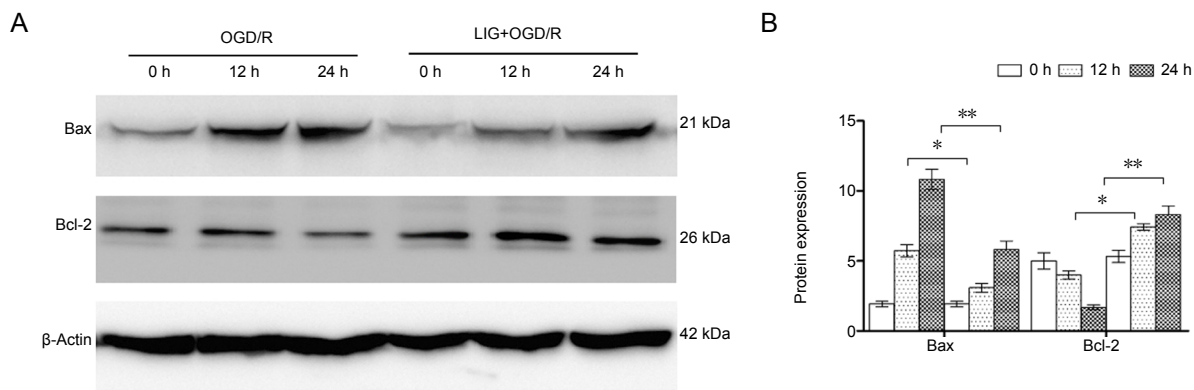


Figure 5 LIG downregulates mitochondrial pathway apoptosis-related proteins in PC12 cells exposed to OGD/R.

(A) Western blotting for apoptosis-related proteins in PC12 cells exposed to OGD/R. (B) Quantitative results. Data are expressed as the mean \pm SD. * $P < 0.05$, ** $P < 0.01$ (one-way analysis of variance followed by Dunnett's test). Experiments were repeated at least three times. LIG: Ligustilide; OGD/R: oxygen-glucose deprivation/reoxygenation.

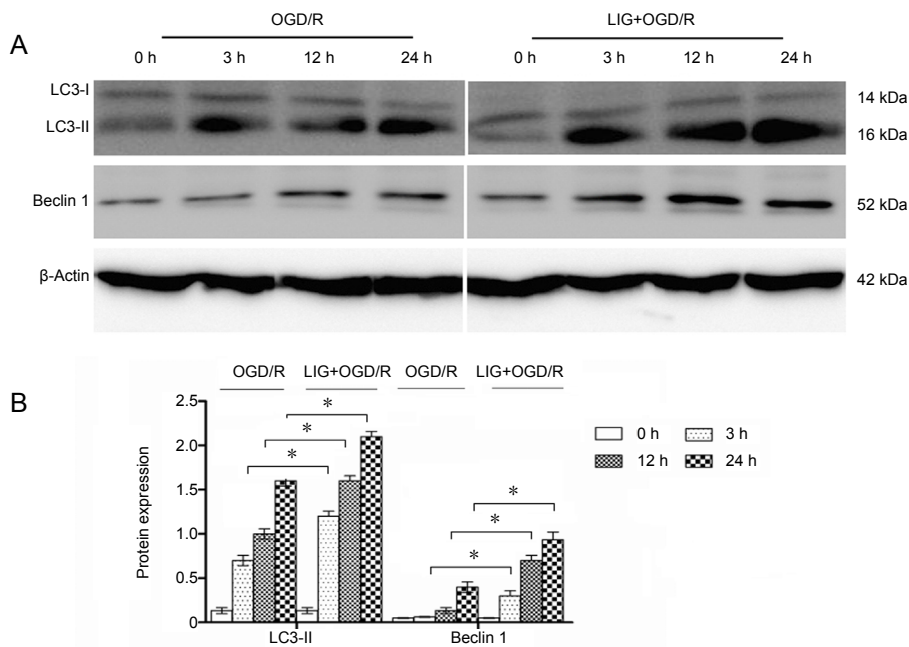


Figure 6 Effect of LIG on autophagy in OGD/R-exposed PC12 cells.

(A) Western blotting was used to measure autophagy-related proteins (LC3-II and Beclin 1) in PC12 cells exposed to OGD/R. (B) Quantitative results of protein expression. Data are expressed as the mean \pm SD. * $P < 0.05$ (one-way analysis of variance followed by Dunnett's test). Experiments were repeated at least three times. LC3-II: Microtubule-associated protein I light chain 3B; LIG: ligustilide; OGD/R: oxygen-glucose deprivation/reoxygenation.

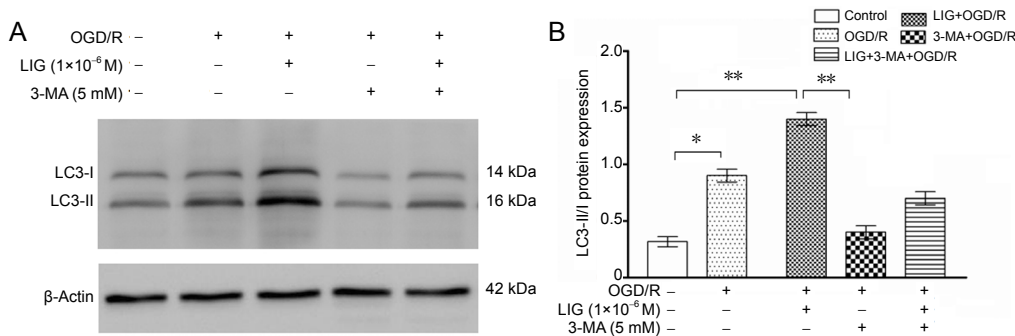


Figure 7 LIG increases LC3-II expression and upregulates autophagy.

(A) Western blot was used to detect levels of the autophagy-related protein LC3-II. (B) Quantitative results of protein expression. Data are expressed as the mean \pm SD. * $P < 0.05$, ** $P < 0.01$ (one-way analysis of variance followed by Dunnett's test). Experiments were repeated at least three times. 3-MA: 3-Methyladenine; LC3-II: microtubule-associated protein I light chain 3B; LIG: ligustilide; OGD/R: oxygen-glucose deprivation/reoxygenation.

R-induced apoptosis of these cells. Bcl-2 inhibits apoptosis and Bax promotes apoptosis (Cregan et al., 1999; Renault et al., 2013). Here, Bcl-2 protein expression was decreased in PC12 cells exposed to OGD/R. In contrast, Bax expression was robustly increased, and these effects were significantly reversed by LIG treatment. This suggests that LIG inhibits apoptosis in PC12 cells by upregulating Bcl-2 and downregulating Bax.

Autophagy has a dual role—it is not only cytoprotective, but can also lead to cell death (Li et al., 2015). In the central nervous system, autophagy serves as a survival-promoting pathway to protect cells from cerebral ischemia (Han et al., 2012; He et al., 2019). For example, sirtuin 3 exerts a neuroprotective effect by promoting autophagy (Majd et al., 2018). LC3-II is a marker of autophagy (Dai et al., 2017). Beclin 1 regulates other autophagic proteins attached to the autophagosomal membrane and reduces the accumulation of LC3-II (Su et al., 2015). The autophagy index, the LC3-II/LC3-I ratio, is upregulated in the hypoxic-ischemic brain (Deng et al., 2013; Schläfli et al., 2015). We found here that the LC3-II/LC3-I ratio and Beclin 1 expression increased in PC12 cells after hypoxia treatment, but the upregulation was limited. After LIG treatment, Beclin 1 and LC3-II protein expression in OGD/R-exposed PC12 cells increased substantially. Along with the increase in autophagy, the apoptosis rate decreased significantly. 3-MA significantly downregulated autophagy, accompanied by an increase in the apoptosis rate. Together with the electron microscopy images and immunofluorescence results, these results strongly suggest that LIG protects neuronal cells by enhancing autophagy.

AMPK acts on mTOR kinase, thereby upregulating autophagy (Liu et al., 2018). Several upstream kinases, including LKB1, activate AMPK by phosphorylation (Zhang et al., 2018). Activation of the AMPK/mTOR pathway is involved in neural cell apoptosis and autophagy (Li et al., 2017a). Additionally, sirtuin 3 promotes autophagy to protect neural cells through the LKB1-AMPK-mTOR pathway (Majd et al., 2018). Here, we found that the LKB1-AMPK-mTOR pathway is activated by LIG to promote autophagy in OGD/R-exposed cells. We used the autophagy inhibitor 3-MA or the AMPK inhibitor dorsomorphin to clarify the relationship between the LKB1-AMPK-mTOR signaling pathway and apoptosis. After treatment with 3-MA or dorsomorphin, phosphorylation of LKB1 and AMPK was inhibited, phosphorylation of mTOR was increased, and the protective effect of LIG was diminished.

In summary, LIG inhibited apoptosis in the PC12 cell model of ICI by upregulating autophagy. LIG increased the LC3-II/LC3-I ratio, Beclin 1 protein expression, and the formation of autophagosomes. Moreover, LIG induced the activation of the LKB1-AMPK-mTOR autophagy signaling pathway in PC12 cells. Together, these findings suggest that LIG exerts a neuroprotective effect against ischemia-reperfusion injury by promoting autophagy via activation of the LKB1-AMPK-mTOR signaling pathway.

There are some limitations to this study. First, we focused on the role of autophagy in the neuroprotective effect of LIG. The pathogenesis of ICI is highly complex, and other pathological mechanisms likely contribute to cell and tissue dam-

age. The neuroprotective effect of LIG may therefore involve the regulation of non-autophagy processes as well. Further study is needed to more fully clarify the neuroprotective mechanisms of LIG. However, effective clinical treatment of ICI is currently lacking. LIG, the active ingredient of a traditional Chinese medicine, is derived from a renewable natural resource and has low toxicity. Our findings suggest that it may have therapeutic potential for the clinical management of ICI.

Acknowledgments: Thanks for Dr. Dong-Yu Min (Experimental Center of Affiliated Hospital of Liaoning University of Traditional Chinese Medicine, Shenyang, China) providing the PC12 cells.

Author contributions: Study design, data acquisition and interpretation: DYZ, GRB; experimental implementation: DDY; manuscript drafting and revising: DYZ, LR; study supervising: GRB. All authors approved the final version of the paper.

Conflicts of interest: There were no conflicts of interest in this experiment.

Financial support: None.

Institutional review board statement: The study did not involve ethical issues.

Copyright license agreement: The Copyright License Agreement has been signed by all authors before publication.

Data sharing statement: Datasets analyzed during the current study are available from the corresponding author on reasonable request.

Plagiarism check: Checked twice by iThenticate.

Peer review: Externally peer reviewed.

Open access statement: This is an open access journal, and articles are distributed under the terms of the Creative Commons Attribution-Non-Commercial-ShareAlike 4.0 License, which allows others to remix, tweak, and build upon the work non-commercially, as long as appropriate credit is given and the new creations are licensed under the identical terms.

Open peer reviewer: Sergei Fedorovich, Institute of Biophysics and Cell Engineering, National Academy of Sciences of Belarus, Belarus.

References

- Ahn JY, Rong R, Kroll TG, Van Meir EG, Snyder SH, Ye K (2004) PIKE (phosphatidylinositol 3-kinase enhancer)-A GTPase stimulates Akt activity and mediates cellular invasion. *J Biol Chem* 279:16441-16451.
- Byun EB, Park WY, Kim WS, Song HY, Sung NY, Byun EH (2018) Neuroprotective effect of Capsicum annuum var. abbreviatum against hydrogen peroxide-induced oxidative stress in HT22 hippocampus cells. *Biosci Biotechnol Biochem* 82:2149-2157.
- Cregan SP, MacLaurin JG, Craig CG, Robertson GS, Nicholson DW, Park DS, Slack RS (1999) Bax-dependent caspase-3 activation is a key determinant in p53-induced apoptosis in neurons. *J Neurosci* 19:7860-7869.
- Dai R, Zhang S, Duan W, Wei R, Chen H, Cai W, Yang L, Wang Q (2017) Enhanced autophagy contributes to protective effects of GM1 ganglioside against abeta1-42-induced neurotoxicity and cognitive deficits. *Neurochem Res* 42:2417-2426.
- Deng YN, Shi J, Liu J, Qu QM (2013) Celastrol protects human neuroblastoma SH-SY5Y cells from rotenone-induced injury through induction of autophagy. *Neurochem Int* 63:1-9.
- Descloux C, Ginet V, Clarke PG, Puyal J, Truttmann AC (2015) Neuronal death after perinatal cerebral hypoxia-ischemia: Focus on autophagy-mediated cell death. *Int J Dev Neurosci* 45:75-85.
- Ecker N, Mor A, Journo D, Abeliovich H (2010) Induction of autophagic flux by amino acid deprivation is distinct from nitrogen starvation-induced macroautophagy. *Autophagy* 6:879-890.
- Fan J, Liu Y, Yin J, Li Q, Li Y, Gu J, Cai W, Yin G (2016) Oxygen-glucose-deprivation/reoxygenation-induced autophagic cell death depends on JNK-mediated phosphorylation of Bcl-2. *Cell Physiol Biochem* 38:1063-1074.
- Fayaz SM, Suvanish Kumar VS, Rajanikant GK (2014) Necroptosis: who knew there were so many interesting ways to die? *CNS Neurol Disord Drug Targets* 13:42-51.
- Gabryel B, Kost A, Kasprowska D (2012) Neuronal autophagy in cerebral ischemia—a potential target for neuroprotective strategies? *Pharmacol Rep* 64:1-15.
- Han J, Pan XY, Xu Y, Xiao Y, An Y, Tie L, Pan Y, Li XJ (2012) Curcumin induces autophagy to protect vascular endothelial cell survival from oxidative stress damage. *Autophagy* 8:812-825.

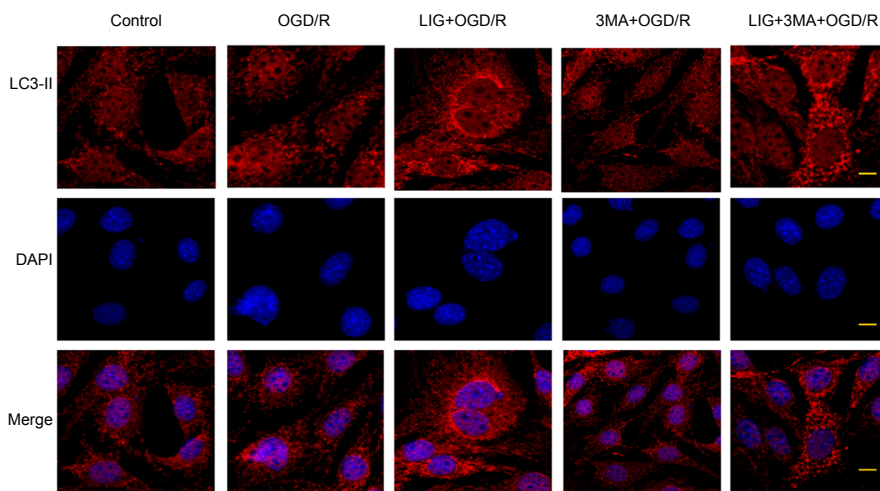


Figure 8 Effect of LIG on autophagosomes in PC12 cells exposed to OGD/R.

Accumulation of LC3-II (Cy3, red) around the nucleus followed OGD/R exposure for 12 hours, and the expression and distribution of LC3-II was clearly amplified by administration of LIG. 3-MA, with or without LIG, reduced the expression of LC3-II. Scale bars: 0.5 μm. 3-MA: 3-Methyladenine; LC3-II: microtubule-associated protein 1 light chain 3B; LIG: ligustilide; OGD/R: oxygen-glucose deprivation/reoxygenation.

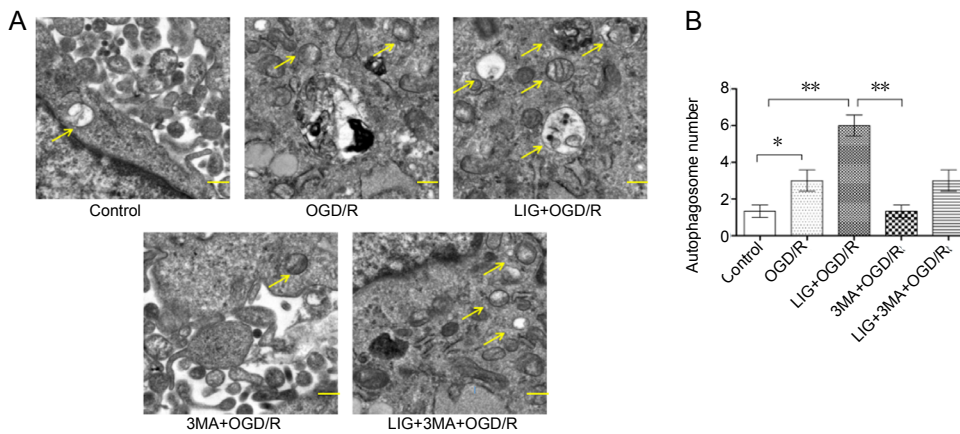


Figure 9 LIG increases the formation of autophagosomes in OGD/R-exposed PC12 cells.

(A) Transmission electron microscopy was used to examine the structure of the autophagosomes (yellow arrows). Scale bars: 0.5 μm. (B) Quantitative results of protein expression. Data are expressed as the mean ± SD. * $P < 0.05$, ** $P < 0.01$ (one-way analysis of variance followed by Dunnett's test). Experiments were repeated at least three times. 3-MA: 3-Methyladenine; LIG: ligustilide; OGD/R: oxygen-glucose deprivation/reoxygenation.

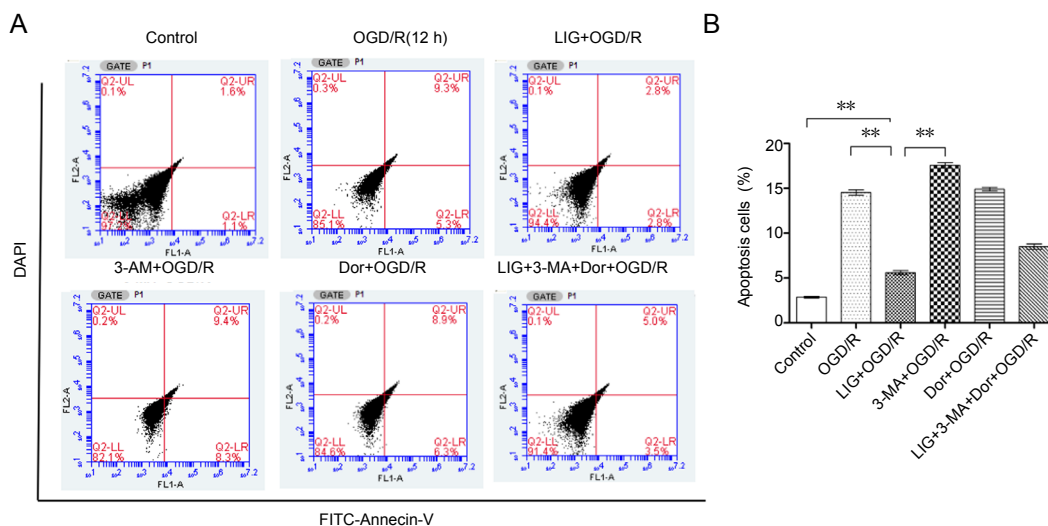


Figure 10 LIG attenuates OGD/R-induced apoptosis by upregulating autophagy.

(A) Flow cytometry for detecting PC12 cell apoptosis. (B) Quantitative results of the apoptotic data. Data are expressed as the mean ± SD. ** $P < 0.01$ (one-way analysis of variance followed by Dunnett's test). Experiments were repeated at least three times. 3-MA: 3-Methyladenine; Dor: dorsomorphin; LIG: ligustilide; OGD/R: oxygen-glucose deprivation/reoxygenation.

He HY, Ren L, Guo T, Deng YH (2019) Neuronal autophagy aggravates microglial inflammatory injury by downregulating CX3CL1/fractalkine after ischemic stroke. *Neural Regen Res* 14:280-288.
 Kaverina NV, Kadagidze ZG, Borovjagin AV, Karseladze AI, Kim CK, Lesniak MS, Miska J, Zhang P, Baryshnikova MA, Xiao T, Ornelles D, Cobbs C, Khramtsov A, Ulasov IV (2018) Tamoxifen overrides autophagy inhibition in Beclin 1-deficient glioma cells and their resistance to adenovirus-mediated oncolysis via upregulation of PUMA and BAX. *Oncogene* 37:6069-6082.
 Klein R, Brown D, Turnley AM (2007) Phenoxodiol protects against Cisplatin induced neurite toxicity in a PC-12 cell model. *BMC Neurosci* 8:61.

Komatsu M, Waguri S, Chiba T, Murata S, Iwata J, Tanida I, Ueno T, Koike M, Uchiyama Y, Kominami E, Tanaka K (2006) Loss of autophagy in the central nervous system causes neurodegeneration in mice. *Nature* 441:880-884.
 Kuang X, Yao Y, Du JR, Liu YX, Wang CY, Qian ZM (2006) Neuroprotective role of Z-ligustilide against forebrain ischemic injury in ICR mice. *Brain Res* 1102:145-153.
 Kuang X, Zhou HJ, Thorne AH, Chen XN, Li LJ, Du JR (2017) Neuroprotective effect of ligustilide through induction of alpha-secretase processing of both APP and Klotho in a mouse model of Alzheimer's Disease. *Front Aging Neurosci* 9:353.

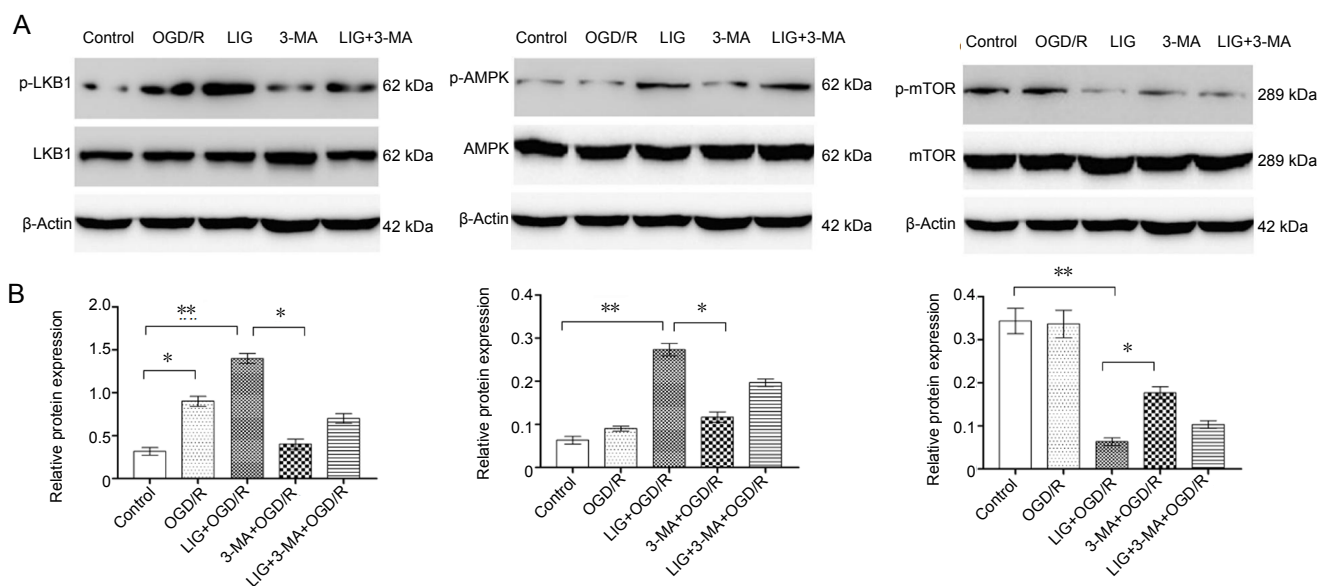


Figure 11 LIG upregulates autophagy through the LKB1-AMPK-mTOR pathway.

(A) Western blotting was used to detect autophagy pathway-related proteins (LKB1, p-LKB1, AMPK, p-AMPK, mTOR and p-mTOR). (B) Quantitative results of p-LKB1, p-AMPK, and p-mTOR protein expression. Results are expressed as the optical density ratio (p-LKB1/LKB1, p-AMPK/AMPK, and p-mTOR/mTOR; mean \pm SD). * P < 0.05, ** P < 0.01 (one-way analysis of variance followed by Dunnett's test). Experiments were repeated at least three times. 3-MA: 3-Methyladenine; AMPK: 5'-adenosine monophosphate-activated protein kinase; Dor: dorsomorphin; LKB1: liver kinase B1; LIG: ligustilide; mTOR: mammalian target of rapamycin; OGD/R: oxygen-glucose deprivation/reoxygenation.

- Li M, Tan J, Miao Y, Lei P, Zhang Q (2015) The dual role of autophagy under hypoxia-involvement of interaction between autophagy and apoptosis. *Apoptosis* 20:769-777.
- Li R, Zhou P, Guo Y, Lee JS, Zhou B (2017a) Tris (1, 3-dichloro-2-propyl) phosphate induces apoptosis and autophagy in SH-SY5Y cells: Involvement of ROS-mediated AMPK/mTOR/ULK1 pathways. *Food Chem Toxicol* 100:183-196.
- Li ZN, Han W, Rong LQ, Gong AP, Lv Y, Shan JJ, Wei XE (2017b) Influence of angiogenesis on neural stem cell proliferation in the subventricular zone after focal cerebral ischemia/reperfusion. *Zhongguo Zuzhi Gongcheng Yanjiu* 21:4697-4702.
- Liu L, Yang L, Chang B, Zhang J, Guo Y, Yang X (2018) The protective effects of rapamycin on cell autophagy in the renal tissues of rats with diabetic nephropathy via mTOR-S6K1-LC3II signaling pathway. *Ren Fail* 40:492-497.
- Long YE, Wang XL, Wang MP, Tang XJ (2019) Effects of androgen on the expression of Bcl-2, Bax and Cyt-C in brain tissue of adult rat models of middle cerebral artery occlusion. *Zhongguo Zuzhi Gongcheng Yanjiu* 23:4344-4349.
- Majd S, Power JHT, Chataway TK, Grantham HJM (2018) A comparison of LKB1/AMPK/mTOR metabolic axis response to global ischaemia in brain, heart, liver and kidney in a rat model of cardiac arrest. *BMC Cell Biol* 19:7.
- Mo ZT, Li WN, Zhai YR, Gao SY (2017) The effects of icariin on the expression of HIF-1 α , HSP-60 and HSP-70 in PC12 cells suffered from oxygen-glucose deprivation-induced injury. *Pharm Biol* 55:848-852.
- Qi H, Jiang Z, Wang C, Yang Y, Li L, He H, Yu Z (2017) Sensitization of tamoxifen-resistant breast cancer cells by Z-ligustilide through inhibiting autophagy and accumulating DNA damages. *Oncotarget* 8:29300-29317.
- Qian HZ, Zhang H, Yin LL, Zhang JJ (2018) Postischemic housing environment on cerebral metabolism and neuron apoptosis after focal cerebral ischemia in rats. *Curr Med Sci* 38:656-665.
- Qiao L, Fu J, Xue X, Shi Y, Yao L, Huang W, Li J, Zhang D, Liu N, Tong X, Du Y, Pan Y (2018) Neuronal injury and roles of apoptosis and autophagy in a neonatal rat model of hypoxia-ischemia-induced periventricular leukomalacia. *Mol Med Rep* 17:5940-5949.
- Rami A, Langhagen A, Steiger S (2008) Focal cerebral ischemia induces upregulation of Beclin 1 and autophagy-like cell death. *Neurobiol Dis* 29:132-141.
- Rana DS, Anand I, Batra A, Sethi PK, Bhargava S (2018) Serum levels of high-sensitivity C-reactive protein in acute ischemic stroke and its subtypes: a prospective case-control study. *Asia Pac J Clin Trials Nerv Syst Dis* 3:128-135.
- Rao E, Zhang Y, Li Q, Hao J, Egilmez NK, Suttles J, Li B (2016) AMPK-dependent and independent effects of AICAR and compound C on T-cell responses. *Oncotarget* 7:33783-33795.
- Renault TT, Teijido O, Antonsson B, Dejean LM, Manon S (2013) Regulation of Bax mitochondrial localization by Bcl-2 and Bcl-x(L): keep your friends close but your enemies closer. *Int J Biochem Cell Biol* 45:64-67.
- Schläfli AM, Berezowska S, Adams O, Langer R, Tschan MP (2015) Reliable LC3 and p62 autophagy marker detection in formalin fixed paraffin embedded human tissue by immunohistochemistry. *Eur J Histochem* 59:2481-2481.
- Shen C, Xian W, Zhou H, Chen L, Pei Z (2016) Potential protective effects of autophagy activated in MPP+ treated astrocytes. *Exp Ther Med* 12:2803-2810.
- Shi Y, Xiao L, Yin Y, Wei L (2015) Ligustilide inhibits tumour necrosis factor-alpha-induced autophagy during C2C12 cells differentiation. *Biomed Pharmacother* 69:42-46.
- Siniscalchi A, Gallelli L, Malferrari G, Pirritano D, Serra R, Santangelo E, De Sarro G (2014) Cerebral stroke injury: the role of cytokines and brain inflammation. *J Basic Clin Physiol Pharmacol* 25:131-137.
- Su X, Wang X, Liu Q, Wang P, Xu C, Leung AW (2015) The role of Beclin 1 in SDT-induced apoptosis and autophagy in human leukemia cells. *Int J Radiat Biol* 91:472-479.
- Suda S, Kimura K (2019) Therapeutic potential of AMPA receptor antagonist perampanel against cerebral ischemia: beyond epileptic disorder. *Neural Regen Res* 14:1525-1526.
- Tobin MK, Bonds JA, Minshall RD, Pelligrino DA, Testai FD, Lazarov O (2014) Neurogenesis and inflammation after ischemic stroke: what is known and where we go from here. *J Cereb Blood Flow Metab* 34:1573-1584.
- Yousuf S, Atif F, Ahmad M, Hoda N, Ishrat T, Khan B, Islam F (2009) Resveratrol exerts its neuroprotective effect by modulating mitochondrial dysfunctions and associated cell death during cerebral ischemia. *Brain Res* 1250:242-253.
- Yu J, Jiang Z, Ning L, Zhao Z, Yang N, Chen L, Ma H, Li L, Fu Y, Zhu H, Qi H (2015) Protective HSP70 induction by Z-ligustilide against oxygen-glucose deprivation injury via activation of the MAPK pathway but not of HSF1. *Biol Pharm Bull* 38:1564-1572.
- Zhang JF, Zhang L, Shi LL, Zhao ZH, Xu H, Liang F, Li HB, Zhao Y, Xu X, Yang K, Tian YF (2017) Parthenolide attenuates cerebral ischemia/reperfusion injury via Akt/GSK-3beta pathway in PC12 cells. *Biomed Pharmacother* 89:1159-1165.
- Zhang M, Deng YN, Zhang JY, Liu J, Li YB, Su H, Qu QM (2018) SIRT3 protects rotenone-induced injury in SH-SY5Y cells by promoting autophagy through the LKB1-AMPK-mTOR pathway. *Aging Dis* 9:273-286.
- Zhu JR, Tao YF, Lou S, Wu ZM (2010) Protective effects of ginsenoside Rb(3) on oxygen and glucose deprivation-induced ischemic injury in PC12 cells. *Acta Pharmacol Sin* 31:273-280.
- Zhu Y, Wang Q, Tang X, Yao G, Sun L (2018) Mesenchymal stem cells enhance autophagy of human intrahepatic biliary epithelial cells in vitro. *Cell Biochem Funct* 36:280-287.

P-Reviewer: Fedorovich S; C-Editor: Zhao M; S-Editors: Yu J, Li CH; L-Editors: Patel B, Yu J, Song LP; T-Editor: Jia Y